Coherent Asymmetric Absorbers

F.S. Cuesta,[1,*] A.D. Kuznetsov,[1,2] G.A. Ptitcyn,[1] X. Wang,[1] and S.A. Tretyakov[1]

[1] *Department of Electronics and Nanoengineering, Aalto University, P.O. Box 15500, Aalto FI-00076, Finland*

[2] *School of Electronic Engineering, HSE University, Tallinskaya Ulitsa, 34, Moscow 123458, Russia*

(Received 10 December 2021; revised 20 January 2022; accepted 31 January 2022; published 24 February 2022)

Most applications of metasurfaces require excitation and control of both electric and magnetic surface currents. For such purposes, the metasurface must have a finite thickness to handle magnetic surface currents. For metasurface sheets of negligible thickness that offer only electric response, coherent illumination can compensate the need to create discontinuities of the tangential electric field component using magnetic surface currents. Most of the known coherent metasurfaces are space uniform and can control only plane-wave absorption and specular reflection. However, it is also known that periodical space-modulated (inhomogeneous) metasurfaces can be used to realize anomalous reflection, refraction, and other useful effects. In this paper, we propose the concept of a coherently illuminated space-modulated metasurface that functions as a coherent asymmetric absorber. We study its behavior under nonideal illumination and suggest applications related to sensing.

DOI: 10.1103/PhysRevApplied.17.024066

I. INTRODUCTION

The first step in designing metasurface devices is to determine the surface impedance that corresponds to the desired scattering for a predefined illumination (see, e.g., Refs. [1,2]). For different design targets, the required properties of the metasurface can be different, requiring chirality (for polarization conversion, for example), time modulation (for frequency conversion or nonreciprocal response), space modulation (for engineering reflection and refraction directions), or other properties. In the case of periodical space modulations, the availability and propagation directions of the nonspecular modes are determined by the period of the surface-impedance variations, as described by the Floquet theory [3]. However, the power distribution between specular and available nonspecular modes is determined by the surface-impedance variation profile [4]. Because of that, space-modulated metasurfaces can produce such effects as anomalous reflection and refraction [2,5–8], retroreflection [9–11], or asymmetric absorption [12].

At the conceptual level, a metasurface behaves as a sheet creating discontinuities of fields or as an impenetrable boundary. If the objective is to control reflection only, metasurfaces are often realized as an impedance sheet above a metallic ground plane, realizing an effective boundary at the plane of the impedance sheet [13]. On the other hand, metasurfaces designed for control of transmission do not have a ground plane, behaving as sheets carrying electric and magnetic surface currents [2]. Many functionalities cannot be realized using sheets supporting only electric surface currents (for microwave applications, usually realized as single arrays of thin metal patches), for example, perfect absorption or retroreflection. In these cases, metasurfaces must carry also magnetic surface currents, which requires the use of at least two parallel arrays or some volumetric particles [14]. However, coherent metasurfaces can produce these desired effects using a secondary illumination source, even if the metasurface sheet is negligibly thin and no magnetic current can be excited [15–21]. Space-modulated metasurface boundaries, realized as finite-size layers carrying both electric and magnetic surface currents, can behave as asymmetric absorbers [12,22–24].

In this paper, we introduce the concept of a space-modulated single-sheet coherent asymmetric absorber: a device that behaves as an absorber or as a retroreflector depending on the angle of incidence of illumination by two coherent waves, as illustrated in Fig. 1. This work focuses on describing how the angle of incidence and variations in the magnitudes and phases of the coherent sources affect the response of the metasurface. In addition, this paper proposes applications where ideal and nonideal coherent illumination can be exploited for sensing and power absorption.

II. COHERENT RETROREFLECTION AND ABSORPTION IN SPACE-MODULATED SHEETS

Let us consider a flat negligibly thin metasurface that divides the space into two regions. The metasurface is

*francisco.cuestasoto@aalto.fi

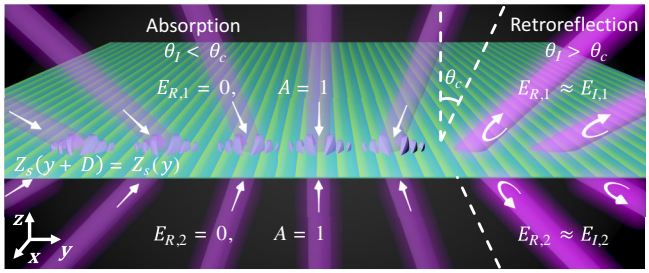

FIG. 1. The concept of a coherent asymmetric absorber, which for different angles of incidence behaves as an absorber or as a reflective surface. The cutoff angle θ_c is determined by the metasurface period.

illuminated by two plane waves at the same angle of incidence θ_I but incident from each region separately. We start the analysis by designing a metasurface-impedance profile that ensures perfect retroreflection of both illuminating waves at the design angle $\theta_I = \theta_{\rm ms}$ (see Fig. 2). The incident waves can be polarized either as transverse-electric (TE) or transverse-magnetic (TM) waves. This paper will focus on TE-illumination scenarios, as shown in Fig. 2(a), but the same principles can be also applied to the TM case, illustrated in Fig. 2(b). The fields for a TE-polarized illumination read

$$\mathbf{E}_{I,1} = E_{I,1} e^{-jk_0[y\sin(\theta_I) - z\cos(\theta_I)]}\mathbf{x},$$
$$\mathbf{H}_{I,1} = -\frac{E_{I,1}}{\eta_0}\Big[\cos(\theta_I)\mathbf{y} + \sin(\theta_I)\mathbf{z}\Big] e^{-jk_0[y\sin(\theta_I) - z\cos(\theta_I)]}, \tag{1}$$

$$\mathbf{E}_{R,1} = -E_{R,1} e^{jk_0[y\sin(\theta_I) - z\cos(\theta_I)]}\mathbf{x},$$
$$\mathbf{H}_{R,1} = -\frac{E_{R,1}}{\eta_0}\Big[\cos(\theta_I)\mathbf{y} + \sin(\theta_I)\mathbf{z}\Big] e^{jk_0[y\sin(\theta_I) - z\cos(\theta_I)]}, \tag{2}$$

in region 1 and

$$\mathbf{E}_{I,2} = E_{I,2} e^{-jk_0[y\sin(\theta_I) + z\cos(\theta_I)]}\mathbf{x},$$
$$\mathbf{H}_{I,2} = \frac{E_{I,2}}{\eta_0}\Big[\cos(\theta_I)\mathbf{y} - \sin(\theta_I)\mathbf{z}\Big] e^{-jk_0[y\sin(\theta_I) + z\cos(\theta_I)]}, \tag{3}$$

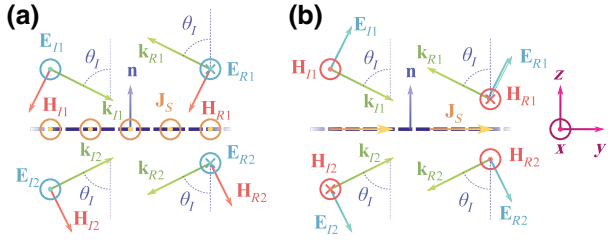

FIG. 2. Incident and reflected plane waves from coherent retroreflective electromagnetic metasurfaces that are designed for (a) transverse-electric and (b) transverse-magnetic polarizations.

$$\mathbf{E}_{R,2} = -E_{R,2} e^{jk_0[y\sin(\theta_I) + z\cos(\theta_I)]}\mathbf{x},$$
$$\mathbf{H}_{R,2} = \frac{E_{R,2}}{\eta_0}\Big[\cos(\theta_I)\mathbf{y} - \sin(\theta_I)\mathbf{z}\Big] e^{jk_0[y\sin(\theta_I) + z\cos(\theta_I)]}, \tag{4}$$

in region 2; where E_I and E_R are the amplitudes of the incident and reflected waves, respectively; k_0 is the wavenumber of the incident waves and η_0 is the characteristic impedance of the surrounding medium. The metasurface must be tailored such that only a single nonspecular mode becomes excited when the metasurface is illuminated at the design angle $\theta_{\rm ms}$. The resulting reflected mode propagates back in the same direction as the incident wave, with a predetermined relative reflection amplitude Γ and phase ϕ_R with respect to the incident waves [$E_{R,1} = E_{I,1}\Gamma\exp(j\,\phi_R)$, $E_{R,2} = E_{I,2}\Gamma\exp(j\,\phi_R)$]. The excess of energy supplied by the sources is absorbed by the metasurface.

The metasurface can be modeled as a sheet of electric surface current density $\mathbf{J}_s = \mathbf{E}/Z_s$, where $\mathbf{E}$ is the tangential component of the macroscopic electric field at the metasurface plane and Z_s is the surface impedance. Since no magnetic surface currents are induced, the metasurface does not produce any discontinuity in the tangential electric field. In this case, symmetric perfect retroreflection can be realized only if both incident waves have the same amplitude and phase ($E_{I,1} = E_{I,2}$), so that the reflected waves also have equal complex amplitudes ($E_{R,1} = E_{R,2}$). Therefore, for a given incidence direction, the surface impedance required for perfect coherent retroreflection can be determined by satisfying the boundary conditions for the total tangential electric and magnetic fields (the electric surface current density is equal to the jump of the tangential magnetic field). For TE or TM illumination, the surface-impedance profiles read, respectively,

$$Z_s^{\rm TE}(y) = \frac{\eta_0}{2\cos\theta_{\rm ms}}\frac{\exp(-2jk_0 y\sin\theta_{\rm ms}) - \Gamma\exp(j\,\phi_R)}{\exp(-2jk_0 y\sin\theta_{\rm ms}) + \Gamma\exp(j\,\phi_R)}, \tag{5a}$$

$$Z_s^{\rm TM}(y) = \frac{\eta_0\cos\theta_{\rm ms}}{2}\frac{\exp(-2jk_0 y\sin\theta_{\rm ms}) + \Gamma\exp(j\,\phi_R)}{\exp(-2jk_0 y\sin\theta_{\rm ms}) - \Gamma\exp(j\,\phi_R)}. \tag{5b}$$

Through inspection, it can be found that the impedance profile is a periodic function with the period $D = \lambda_0/(2\sin\theta_{\rm ms})$, where λ_0 is the reference design wavelength. A change of the reflection phase ϕ_R corresponds to a lateral shift of the impedance position. The continuous impedance profile is usually discretized into enough small subelements with capacitive, inductive, and lossy responses. For microwave applications, the sheet resistance can be implemented using metallic strips, the effective resistance of which is controlled through their width or by meandering them. On the other hand, reactance can be implemented using capacitive gaps or inductive strips [21]. The possibility of independent control of resistance

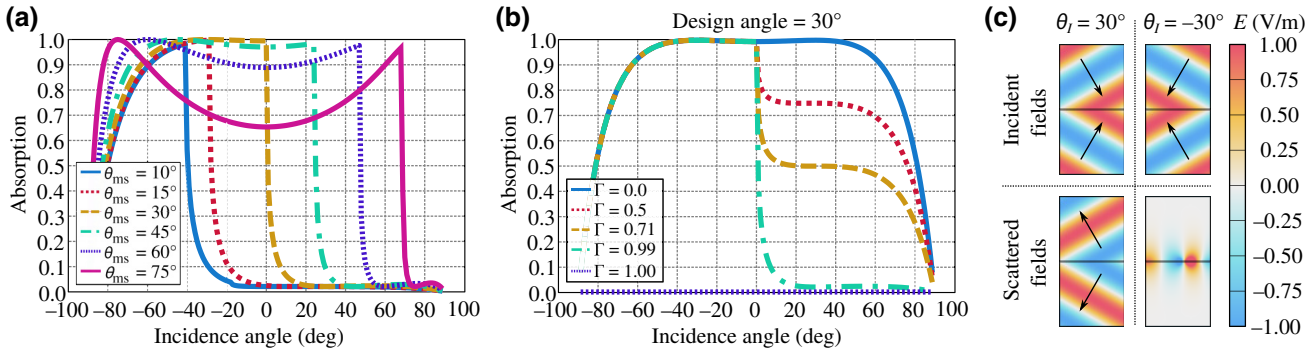

FIG. 3. (a) A metasurface designed to create a nonspecular mode, acting as a retroreflector at the design incidence angle θ_{ms}, has an asymmetric behavior in the form of an absorption region, where nonspecular modes only exist as evanescent waves. This example considers surface impedances corresponding to $\Gamma = 0.99$. (b) In the angular region where the nonspecular mode can propagate, its amplitude can be determined by the reflection coefficient Γ as a design parameter. The structure becomes lossless and symmetric if the value of $|\Gamma| = 1$ is used; however, even for low-loss sheets with the reflection coefficients close to this value, there is strong contrast between the absorption and reflection regions. (c) Numerical simulations in COMSOL show the asymmetric behavior, with near-total retroreflection at the design angle, while the metasurface behaves as an absorber for negative angles of incidence, with evanescent waves localized at the metasurface. These numerical simulations are performed for a surface impedance designed for $\theta_{ms} = 30°$ and $\Gamma = 0.99$.

and reactance has been proved in Ref. [25] and applied in the design of lossy metasurfaces in Refs. [4,12,25]. The surface impedance can be tuned, for example, through the use of varactors and varistors [26]. The implementation of large impedance values is not required as the current flowing through the metasurface is negligibly small.

The numerical results of Fig. 3(a) for coherent retroreflectors with different design angles θ_{ms} reveal that the angular dependence of the absorption is strongly asymmetric. The absorption is high in the angular region, where there is only one propagating mode available (specular reflection), and it is weak where the nonspecular mode is excited as a traveling wave. By changing the design angle of incidence θ_{ms}, it is possible to control these angular regions, delimited by the cutoff angle θ_c. The high-absorption regime mostly corresponds to illumination with "negative" angles of incidence (tilted to the left from the normal to the metasurface plane, as defined in Fig. 2).

This asymmetric behavior allows us to design metasurfaces that exhibit strong coherent retroreflection for positive angles of incidence but strong coherent absorption for negative ones, as illustrated in Fig. 3. An additional design feature is the possibility of controlling the reflection coefficient of the nonspecular mode without disturbing the asymmetric absorption, as portrayed in Fig. 3(b). The asymmetry is present for almost all values of the amplitude of the design reflection coefficient Γ, except for the extreme values $|\Gamma| = 1$ and $\Gamma = 0$, which correspond to already known cases of the perfect coherent retroreflector [21] and the perfect coherent absorber [27], respectively. This asymmetric angular dependence in absorption is similar to the lossy retroreflective boundaries of Ref. [12], illuminated by only one wave.

III. ASYMMETRIC ILLUMINATION

The most attractive feature of coherent metasurfaces is the possibility of tuning the response by varying the phase or amplitude differences between the illuminating waves. To this end, here we analyze the response of coherent retroreflectors illuminated by an arbitrary set of two plane waves. When a sheet designed to function as a coherent retroreflector for a given incidence angle is illuminated by any other source, the reflected field contains infinitely many plane-wave components, as portrayed in Fig. 4. Let us consider a periodical metasurface with the surface impedance Z_s [in particular, given by Eqs. (5a) or (5b)] with the period D, illuminated by a single TE-polarized wave (similar conclusions are achieved for the TM polarization) with an angle of incidence θ_I and wavenumber k. As described by the Floquet theory, the field on the metasurface plane can be considered as a combination of propagating and evanescent plane-wave modes:

$$E = E_I e^{-jyk\sin\theta_i} + \sum_{n=-\infty}^{\infty} E_{[n]} e^{-jyk_{y[n]}}, \tag{6}$$

where $E_{[n]}$ is the amplitude of the nth Floquet harmonic of the field expansion, defined by the wavevector components $k_{y[n]} = k\sin\theta_i + 2\pi n/D$ and $k_{z[n]} = \sqrt{k^2 - k_{y[n]}^2}$. For convenience, we define the mode angle $\theta_{[n]} = \arcsin\left(k_{y[n]}/k\right)$. Note that this angle is imaginary for evanescent components and becomes real at the cutoff angle θ_c, where $k_{y[n]} = |k|$. For the particular case of a coherent asymmetric absorber with the design angle θ_{ms}, the critical angle

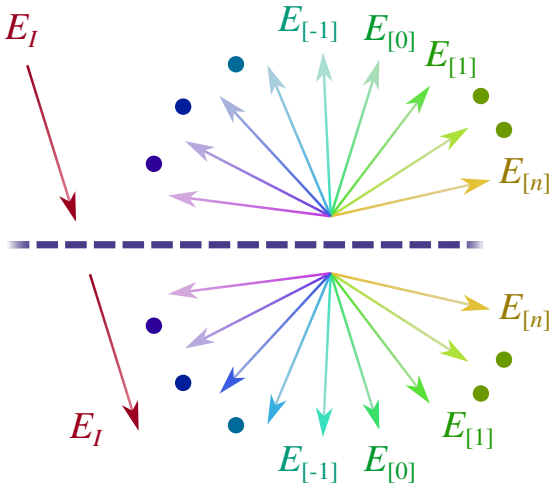

FIG. 4. As described by the Floquet theory, uniform illumination of a periodic surface excites a certain range of specular and nonspecular waves. While the mode range is defined by the period of the surface and the incidence angle of the exciting wave, the amplitude of each excited mode is determined by the surface-impedance profile.

can be found as

$$\theta_c = \arcsin\left(2\sin\theta_{\rm ms} - 1\right). \tag{7}$$

The tangential electric field is continuous across the sheet and the jump of the tangential magnetic field is equal to the surface current density of the induced electric current:

$$\sum_{n=-\infty}^{\infty} 2E_{[n]}\cos\theta_{[n]}e^{-jyk_{y[n]}} = -\eta_0 J_s. \tag{8}$$

Because the sheet response is linear, the current excited by two coherent plane waves can be found as the sum of two independent Floquet expansions corresponding to the two different periods fixed by the two different incidence angles. The boundary condition $Z_s\mathbf{J}_e = \mathbf{E}$ takes the general form

$$\sum_{m=1,2}\sum_{n=-\infty}^{\infty}\left(2\cos\theta_{[n],m} + \frac{\eta_0}{Z_s}\right)E_{[n],m}e^{-jyk_{y[n],m}} = -\frac{\eta_0}{Z_s}\sum_{m=1,2}E_{I,m}e^{-jyk\sin\theta_{i,m}}. \tag{9}$$

In the special case when the two incidence angles are the same, the periods of the two expansions are equal and the two series can be combined into one. For this scenario, Eq. (9) can be rewritten by combining pairs of scattered harmonics ($E_{[n]} = E_{[n],1} + E_{[n],2}$) and the boundary condition takes the form

$$\sum_{n=-\infty}^{\infty}\left(2\cos\theta_{[n]} + \frac{\eta_0}{Z_s}\right)E_{[n]}e^{-jyk_{y[n]}} = -\frac{\eta_0}{Z_s}e^{-jyk\sin\theta_i}\left(E_{I,1} + E_{I,2}\right), \tag{10}$$

where each scattering mode depends not only on the interaction between the fields and the metasurface but also on the direct interaction between the incident waves at the boundary.

In order to understand the effect of the phase-amplitude differences between the two illuminating waves, the amplitude of the source in region 2 can be defined as proportional to that in region 1: $E_{I,2} = E_{I,1}\rho_{I2}\exp(j\,\phi_{I2})$,

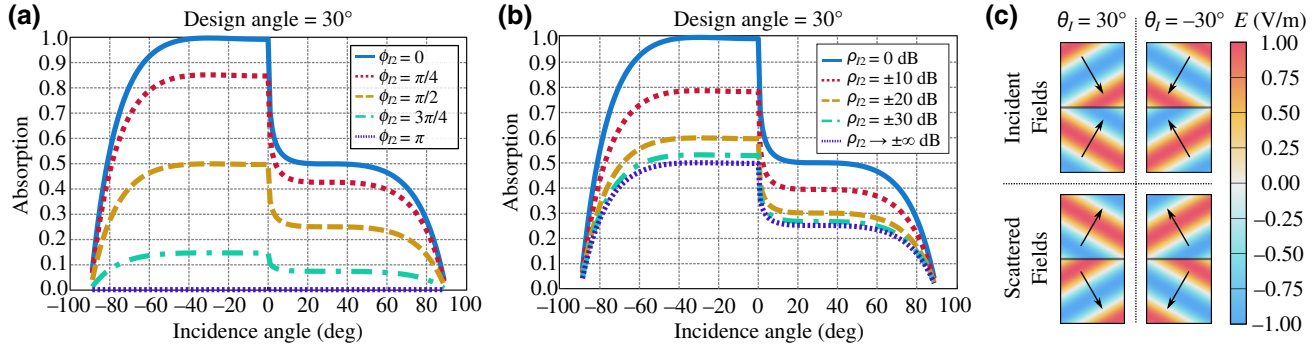

FIG. 5. (a) A coherently illuminated metasurface designed with equivalent electric current densities in mind is matched with the sources when both waves illuminate the surface at the same phase. Any variation in the phase will create a mismatch, leading to some specular reflection. (b) Similarly, the sources are matched with the metasurface as long as both plane waves illuminate the surface with the same amplitude. Any difference in the amplitude breaks the system symmetry, exciting undesired specular reflection. Examples correspond to surface impedances with $\Gamma = 0.71$ and $\theta_{\rm ms} = 30°$. (c) The use of two incident waves with a π phase difference do not excite the coherent metasurface, without producing any scattering. As a result, the incident waves pass through the structure. These numerical results are obtained using COMSOL for a surface impedance designed for $\theta_{\rm ms} = 30°$ and $\Gamma = 0.99$.

where ρ_{I2} is the amplitude ratio. The total incident field at the metasurface plane is then written as

$$E_{\text{tot}} = E_{I,1}\left(1 + \rho_{I2}e^{j\phi_{I2}}\right). \tag{11}$$

The metasurface is functioning as a perfect coherent retroreflector when the two waves have equal amplitudes ($\rho_{I2} = 1$) and phases ($\phi_{I2} = 0$). Otherwise, the metasurface is "mismatched" with respect to the sources and its response can be dramatically different. In the limiting case of the equal amplitude but opposite phase, that is, when $\rho_{I2} = 1$ and $\phi_{I2} = \pi$, the metasurface does not produce any scattering, as shown in Fig. 5(c). In this case, the metasurface behaves as a transparent object (the waves freely pass through the sheet). Thus, in these two limiting cases, the metasurface is either transparent or fully reflective, as a perfect electric conductor boundary (the waves produce total specular reflection, with an additional π phase shift, being in phase with respect to the other incident wave).

IV. NUMERICAL CHARACTERIZATION

The exact values of the scattered-wave amplitudes can be determined for lossless metasurfaces by solving Eq. (9) in combination with the power-conservation law for the propagating modes ($|k_{y[n]}| \leq k$). On the other hand, if the metasurface is lossy or it has an active behavior, power conservation is not usable, as the total scattered power is not equal to the power accepted by the metasurface. For these scenarios, approximate solutions can be found using numerical means based on the Fourier-series expansion of the surface impedance Z_s in combination with the mode-matching method developed in Refs. [4,28]. The absorption in the metasurface is found by subtracting the power reflected into free space from the total incident power.

The results of Fig. 3 show the behavior of the proposed structure with a combination of matching sources, as described in Eq. (11). The strong absorption regime for "negative angles" ($\theta_I < 0$) is achieved by preventing the excitation of the first available nonspecular mode ($n = -1$), leaving only specular reflection ($n = 0$). On the other hand, Figs. 5(a) and 5(b) show how a mismatch between the two coherent sources affects absorption in the metasurface when different phase shifts ϕ_{I2} and amplitude ratios ρ_{I2} are considered, respectively. Obviously, the metasurface behaves as a lossless fully transparent structure when the amplitudes are equal and the phase difference is equal to π. When one of the two amplitudes is much larger than the other, we approach the regime of a single-wave excitation of a sheet of negligible thickness, in which case absorption cannot be higher than 50% of the incident power.

V. POTENTIAL APPLICATIONS OF ASYMMETRIC COHERENT ABSORBERS

Asymmetric absorption and dramatic differences of response of asymmetric coherent absorbers under coherent and incoherent illumination can be exploited in various applications. First, let us consider the setup of Fig. 6(a), where a sample of such a metasurface is placed in the symmetry plane of a parallel-plate waveguide, supporting the TE_1 mode. The field of this mode can be decomposed into two coherent plane waves [29]. By changing the separation between the plates h, the angle of incidence of these partial waves on the metasurface can be tuned. In the considered example, the metasurface is designed with $\theta_{\text{ms}} = 30^\circ$ ($\theta_c = 0^\circ$) and $\Gamma = 0.99$, resulting in high reflection for positive angles and strong absorption for the opposite tilt, as shown in Fig. 3(a). In this configuration, the waveguide inherits the properties of the metasurface as a retroreflector or as an absorber, depending on which end of the waveguide is excited, as portrayed in Figs. 6(b) and 6(c). This behavior is stable over a wide frequency

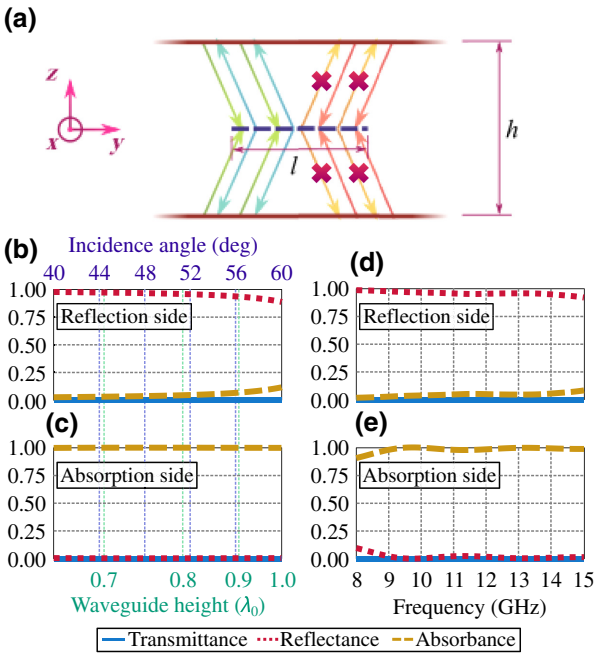

FIG. 6. (a) By inserting a coherent asymmetric absorber inside a parallel-plate waveguide, it is expected to transfer its properties into the waveguide for TE_1 mode. The incidence angle of the TE_1 mode can be controlled by changing the distance between the waveguide plates, as shown in (b) and (c), or by changing the frequency, portrayed in (d) and (e). (b),(d) If the metasurface is designed for $\theta_{\text{ms}} = 30^\circ$, one end of the waveguide becomes highly reflective. (c),(e) On the other hand, the waveguide absorbs the TE_1 wave when it is fed from the opposite end of the waveguide. For this example, the metasurface is designed with $\theta_{\text{ms}} = 30^\circ$, $\Gamma = 0.99$, for a reference frequency of 10 GHz and with a total length of $l = 10D$.

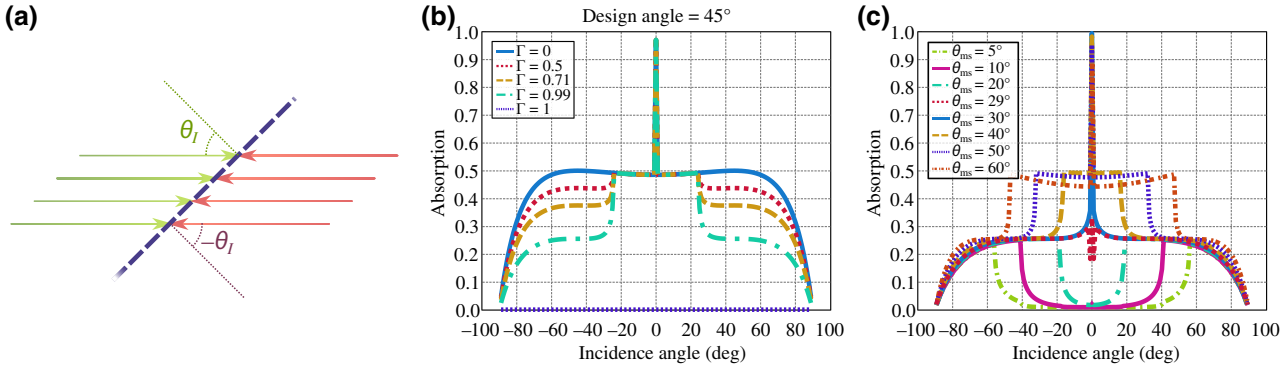

FIG. 7. The positioning of a coherent asymmetric absorber in the field of two counterpropagating plane waves allows us to obtain a structure that is capable of sensing small changes in the metasurface angular position. Coherent illumination at the same angle is realized only for normal incidence ($\theta_I = 0$), in which case the absorption is total. Absorption for any non-normal illumination is comparable to the single-source scenario, where the absorption is limited to 50% of the incident power. (a) The geometry of the setup. (b),(c) The angular dependence of the absorption at oblique illumination can be controlled by tuning $\theta_{\rm ms}$ and Γ. The example in (b) is for the design angle $\theta_{\rm ms} = 45^\circ$ and varying Γ, while (c) is for the reflection coefficient of $\Gamma = 0.99$ and a variable design angle.

range where higher-order modes beyond TE_1 cannot propagate, as is seen in Figs. 6(d) and 6(e). However, close to the cutoff frequency of the TE_1 mode, the response is affected by the difference between the waveguide characteristic impedance with and without the metasurface, resulting in high reflection from both sides. Let us note that this setup does not break reciprocity and transmission through the device is symmetric.

We see that this configuration functions as a compact and broadband microwave absorber in a waveguide that does not contain any terminating boundary and can freely pass high-frequency electromagnetic radiation or, for example, the flow of air or water. Also, for wave propagation in the opposite direction, the device works as a broadband reflector, although there is no reflecting wall.

The second application exploits the fact that for any mismatched illumination, the absorption is limited to 50% of the incident power, while it can be perfect at coherent and symmetric illumination. The sources (or one source and a uniform mirror) are aligned so that the two incident waves propagate in the opposite directions, forming a standing wave. The metasurface is positioned in the field of this standing wave with a tilt with respect to the propagation axis, as illustrated in Fig. 7(a). From the point of view of the metasurface, one of the sources illuminates it at a positive angle of incidence θ_I, while the other wave has a negative angle of incidence $-\theta_I$. Thus, the condition of coherent illumination that requires equal incidence angles for both waves is not fulfilled. The only exception, when the metasurface receives matched illumination, is the case of the normal incidence $\theta_I = 0$. At this singular value of the tilt angle, the absorption is perfect, as shown in Figs. 7(b) and 7(c). For any other angle of incidence, the absorption level drops to 50% or less [see Fig. 3]. The profile, shown in Fig. 7(b), is symmetric, as either both waves illuminate in the absorption regime or one of them excites the nonspecular mode. The absorption level for angles compatible with nonspecular reflection can be controlled using the parameter Γ, down to 25% of the total incident power. The angular range of these regions of different absorption can be controlled through the design angle $\theta_{\rm ms}$, as shown in Fig. 7(c). The case when the metasurface is designed for $\theta_{\rm ms} = 30^\circ$ deserves special attention, as the nonspecular mode can only be excited as a propagating wave for positive angles of incidence θ_I. As a result, considering a reflection coefficient value of $\Gamma = 0.99$, the difference between the absorption peak at normal illumination and the absorption at oblique illumination is maximized.

VI. CONCLUSIONS

In this paper, we present the concept of a coherent asymmetric absorber that changes its behavior according to the incidence angle of coherent-wave illumination. It is shown that negligibly thin nonuniform sheets characterized by the determined sheet impedance operate as coherent counterparts of asymmetric absorbers. Under coherent illumination by two plane waves, the absorption changes from nearly perfect to very small when the incidence angle varies. The study of arbitrary illumination of these sheets reveals how reflection and absorption can be tuned by changing the amplitude and phase of one of the two illuminating waves.

Furthermore, this paper proposes two applications of coherent asymmetric absorbers: as broadband asymmetric waveguide absorbers and as sensors of angular position. By placing a coherent asymmetric absorber sheet inside a parallel-plate waveguide, equidistant from its walls, it is

possible to realize broadband absorption without the need to block the cross-section opening of the waveguide.

By exploiting the dramatic difference between the achievable absorption under perfect coherent illumination by two waves with the same incidence angle and any other kinds of illumination, we show that it is possible to detect angular displacements of objects with extreme accuracy.

ACKNOWLEDGMENTS

This work was supported in part by the Academy of Finland under Grant No. 330260.

[1] F. Yang, Y. Rahmat-Samii, Eds., *Surface Electromagnetics, With Applications in Antenna, Microwave, and Optical Engineering*. Cambridge University Press, 2019.

[2] C. Simovski and S. Tretyakov, *An Introduction to Metamaterials and Nanophotonics* (Cambridge University Press, New York, NY, 2020).

[3] A. Ishimaru, *Periodic Structures and Coupled-Mode Theory*. John Wiley & Sons, Ltd, (2017), ch. 7, p. 201.

[4] X. Wang, A. Díaz-Rubio, and S. A. Tretyakov, Independent Control of Multiple Channels in Metasurface Devices, Phys. Rev. Appl. **14**, 024089 (2020).

[5] Z. Li, L. Huang, K. Lu, Y. Sun, and L. Min, Continuous metasurface for high-performance anomalous reflection, Appl. Phys. Express **7**, 112001 (2014).

[6] K. Tang, C. Qiu, M. Ke, J. Lu, Y. Ye, and Z. Liu, Anomalous refraction of airborne sound through ultrathin metasurfaces, Sci. Rep. **4**, 6517 (2014).

[7] A. Díaz-Rubio, V. S. Asadchy, A. Elsakka, and S. A. Tretyakov, From the generalized reflection law to the realization of perfect anomalous reflectors, Sci. Adv. **3**, e1602714 (2017).

[8] D. Sell, J. Yang, E. W. Wang, T. Phan, S. Doshay, and J. A. Fan, Ultra-high-efficiency anomalous refraction with dielectric metasurfaces, ACS Photonics **5**, 2402 (2018).

[9] Y. Jia, J. Wang, Y. Li, Y. Pang, J. Yang, Y. Fan, and S. Qu, Retro-reflective metasurfaces for backscattering enhancement under oblique incidence, AIP Adv. **7**, 105315 (2017).

[10] V. S. Asadchy, A. Díaz-Rubio, S. N. Tcvetkova, D.-H. Kwon, A. Elsakka, M. Albooyeh, and S. A. Tretyakov, Flat Engineered Multichannel Reflectors, Phys. Rev. X **7**, 031046 (2017).

[11] X. Li, C. Tao, L. Jiang, and T. Itoh, in *2018 48th European Microwave Conference (EuMC)*, (2018), p. 133.

[12] X. Wang, A. Díaz-Rubio, V. S. Asadchy, G. Ptitcyn, A. A. Generalov, J. Ala-Laurinaho, and S. A. Tretyakov, Extreme Asymmetry in Metasurfaces via Evanescent Fields Engineering: Angular-Asymmetric Absorption, Phys. Rev. Lett. **121**, 256802 (2018).

[13] S. Tretyakov, *Analytical Modeling in Applied Electromagnetics* (Artech House, Norwood, MA, 2003).

[14] V. S. Asadchy, I. A. Faniayeu, Y. Ra'di, S. A. Khakhomov, I. V. Semchenko, and S. A. Tretyakov, Broadband Reflectionless Metasheets: Frequency-Selective Transmission and Perfect Absorption, Phys. Rev. X **5**, 031005 (2015).

[15] W. Lv, J. Bing, Y. Deng, D. Duan, Z. Zhu, Y. Li, C. Guan, and J. Shi, Polarization-controlled multifrequency coherent perfect absorption in stereometamaterials, Opt. Express **26**, 17236 (2018).

[16] X. Feng, J. Zou, W. Xu, Z. Zhu, X. Yuan, J. Zhang, and S. Qin, Coherent perfect absorption and asymmetric interferometric light-light control in graphene with resonant dielectric nanostructures, Opt. Express **26**, 29183 (2018).

[17] J. Zou, F. Xiong, J. Zhang, and Z. Zhu, Coherent perfect absorption in artificially engineered nanometer metal/semiconductor composite films at oblique incidence, OSA Continuum **2**, 3251 (2019).

[18] D. G. Baranov, A. Krasnok, T. Shegai, A. Alù, and Y. Chong, Coherent perfect absorbers: Linear control of light with light, Nat. Rev. Mater. **2**, 17064 (2017).

[19] G. Nie, Q. Shi, Z. Zhu, and J. Shi, Selective coherent perfect absorption in metamaterials, Appl. Phys. Lett. **105**, 201909 (2014).

[20] C. A. Valagiannopoulos, F. Monticone, and A. Alù, PT-symmetric planar devices for field transformation and imaging, J. Opt. **18**, 044028 (2016).

[21] F. S. Cuesta, G. A. Ptitcyn, M. S. Mirmoosa, and S. A. Tretyakov, Coherent retroreflective metasurfaces, Phys. Rev. Res. **3**, L032025 (2021).

[22] A. Song, J. Li, X. Peng, C. Shen, X. Zhu, T. Chen, and S. A. Cummer, Asymmetric Absorption in Acoustic Metamirror Based on Surface Impedance Engineering, Phys. Rev. Appl. **12**, 054048 (2019).

[23] X. Wang, X. Fang, D. Mao, Y. Jing, and Y. Li, Extremely Asymmetrical Acoustic Metasurface Mirror at the Exceptional Point, Phys. Rev. Lett. **123**, 214302 (2019).

[24] S. Dong, G. Hu, Q. Wang, Y. Jia, Q. Zhang, G. Cao, J. Wang, S. Chen, D. Fan, W. Jiang, Y. Li, A. Alù, and C.-W. Qiu, Loss-assisted metasurface at an exceptional point, ACS Photonics **7**, 3321 (2020).

[25] X. Wang, A. Díaz-Rubio, A. Sneck, A. Alastalo, T. Mäkelä, J. Ala-Laurinaho, J.-F. Zheng, A. V. Räisänen, and S. A. Tretyakov, Systematic design of printable metasurfaces: Validation through reverse-offset printed millimeter-wave absorbers, IEEE Trans. Antennas Propagation **66**, 1340 (2018).

[26] F. Liu, O. Tsilipakos, A. Pitilakis, A. C. Tasolamprou, M. S. Mirmoosa, N. V. Kantartzis, D.-H. Kwon, J. Georgiou, K. Kossifos, M. A. Antoniades, M. Kafesaki, C. M. Soukoulis, and S. A. Tretyakov, Intelligent Metasurfaces with Continuously Tunable Local Surface Impedance for Multiple Reconfigurable Functions, Phys. Rev. Appl. **11**, 044024 (2019).

[27] Y. Fan, F. Zhang, Q. Zhao, Z. Wei, and H. Li, Tunable terahertz coherent perfect absorption in a monolayer graphene, Opt. Lett. **39**, 6269 (2014).

[28] X. Wang, A. Díaz-Rubio, H. Li, S. A. Tretyakov, and A. Alù, Theory and Design of Multifunctional Space-Time Metasurfaces, Phys. Rev. Appl. **13**, 044040 (2020).

[29] D. M. Pozar, *Microwave Engineering* (Wiley, Hoboken, NJ, 2004), 3rd ed.